

# Effect of pH on hydrogen pick-up and corrosion in Zircaloy-4

James Sayers<sup>1</sup>, Sergio Lozano-Perez<sup>1</sup>, Susan Ortner<sup>2</sup>

1. Department of Materials, University of Oxford, Parks Road, Oxford, UK

2. National Nuclear Laboratory, Building D5, Culham Science Centre, Abingdon, Oxfordshire OX14 3DB UK

**Abstract.** Thermal Desorption Spectroscopy (TDS) has been used to investigate the hydrogen pick-up behaviour in different samples of Zircaloy-4. This includes as-received, cold rolled, hydrogen charged, and autoclave-oxidised in pure water and at an elevated pH (with 50% deuterated water) compared to commercial reactors. A characteristic desorption peak for hydrogen has been found at ~650°C, which is theorised to come from hydrides<sup>1</sup>. Cold rolled samples show the same general shape spectrum as the as-received samples, with more hydrogen detected per unit volume of sample. This suggests more hydrogen is in trapping sites or outward diffusion paths are facilitated by dislocations, since no more hydrogen has been added. The peak broadens towards higher temperature, which indicates that additional dislocations could provide trapping sites with a slightly higher energy than the average in the as-received samples. The hydrogen charged samples form a hydride rim, which contains much more hydrogen than the as-received samples. The peak broadens but on average does not shift.

The surface oxide, when present, layer acts as a barrier to the desorption of hydrogen, until the temperature rises enough for the oxygen to migrate into the bulk. The oxide itself only contains a small amount of hydrogen, as is evidenced when the oxide layer is removed, whereupon the desorption peak returns to the characteristic shape seen in as-received samples.

Samples oxidised in pure water exhibit a slightly higher oxidation rate, and pass through kinetic transition much earlier than samples exposed to an elevated pH. Before transition, pH has little effect on the hydrogen pick-up. After transition, the hydrogen pick-up is much higher in pure water, which implies that the H<sup>+</sup> concentration in the environment affects hydrogen pickup at this stage. The elevated pH samples showed peaks for D-H and D<sub>2</sub>, which follow the H<sub>2</sub> peaks. The hydrogen content in these samples increases at around 70% of the time to the first transition. This may correlate with development of through-thickness percolation paths, which could lead to the pH inside cracks being modified to a lower value, increasing the availability of H<sup>+</sup> ions.

**Keywords:** Zircaloy-4, Hydrogen, Deuterium, Desorption, Trapping

## INTRODUCTION

Zirconium and its alloys are used as nuclear fuel cladding. Understanding the corrosion and hydrogen pick-up of Zr alloys is important as these factors can limit fuel lifetime. Zircaloy-4 was developed after the earlier nickel containing Zircaloy-2 was found to absorb large amounts of hydrogen<sup>2,3</sup>.

Hydrogen generated during oxidation can form hydrogen gas and diffuse into the coolant or it can migrate through the oxide and enter the metal. When hydrogen is absorbed, it forms various zirconium hydrides, which can cause cladding embrittlement<sup>4</sup>. Several different factors can influence hydrogen pick-up, such as the hydrogen and oxygen content of the corrosion media, the composition of the alloy<sup>5</sup>, the temperature, pressure and pH<sup>6</sup>. It has also been found

that hydrogen pick-up can vary with the oxide thickness<sup>5,7</sup>. The ratio of hydrogen absorbed to the hydrogen generated during corrosion is known as the hydrogen pick-up fraction. As summarised by Garzarolli and Cox<sup>6</sup>, there are several mechanisms by which the hydrogen can pass through the oxide:

- Diffusion through the oxide lattice (as protons or OH<sup>-</sup>).
- Migration via pores in the oxide.
- Transport of H through oxidised second phase particles (SPPs).
- Transport of H through non-oxidised SPPs.

As stated by the authors however, 'The mechanism governing the H ingress process is not really known'.

TDS is used to analyse gases which are desorbed from a material. Studies of zirconium have shown that hydrogen desorption occurs at around 650°C<sup>1,8</sup>, and that zirconium oxide acts as a barrier to hydrogen desorption<sup>9-11</sup>. This is thought to be due to the formation of O-H bonds forming in the oxide.<sup>1,8,12</sup>

## **EXPERIMENTAL**

The experiments were carried out using a Hiden Analytical TPD (Thermal Programmed Desorption) workstation. 10mm x 10mm x 1mm samples were placed on an aluminium nitride wafer on top of the heating stage. The wafer prevented the sample sticking to the stage. The sample and wafer are held in place by two pins to ensure good thermal contact between the sample and the heater (shown in Figure 1). The heater can be programmed to follow a particular profile up to 1000°C. The temperature of the sample surface was measured using a pyrometer, and typically reached about 800°C due to the temperature gradient across the AlN wafer. A heating rate of 10°C/min was decided upon as it allows the sample to heat evenly throughout so that any gases measured can be attributed to the temperature given.

A residual gas analyser is used to measure the desorbed gases and can measure from 1 to 50 amu. The emission current of the detector ranges from 1-20 µA, and is raised to increase detection sensitivity.

All the samples reported on were made from Zircaloy-4. Sheets of Zircaloy-4 provided by Westinghouse, were cut into samples used in the calibration tests, for cold-rolling and for the elevated pH exposures. Calibration tests consisted of altering the heating rate and the emission current of the detector to determine the relationships between these settings and the spectra observed. Cold rolled samples were tested to see if adding deformation affected hydrogen desorption.



Figure 1 - View inside the main chamber. 1 - Heater, 2 – Transfer Rod, 3 - Holding pins

AMEC provided three samples hydrogen charged for 5, 24 and 48 hours. SEM images show most of the hydrogen in these samples was located in a hydride rim 10-20 µm from the surface.

Three samples oxidised in an autoclave in pure water at 360°C for 7, 45 and 120 days ( $\text{pH}_{360} = 6.15$ ) were provided through the MUZIC-2 collaboration. They were compared with samples exposed to 50% heavy water, containing 2 ppm Li, 95 ppm K and 1050 ppm B at 350°C ( $\text{pH}_{350} = 8.82$ ), to show the effects of pH on hydrogen pick-up.

shows the oxidation curve for samples oxidized in pure water and at elevated pH. It can be seen that the oxidation rate is reduced in an elevated pH environment, and that transition is delayed (around 120 days for elevated pH compared to 70-90 for the pure water samples). **Error! Reference source not found.** shows the oxidation data for the samples oxidised in the elevated pH environment.

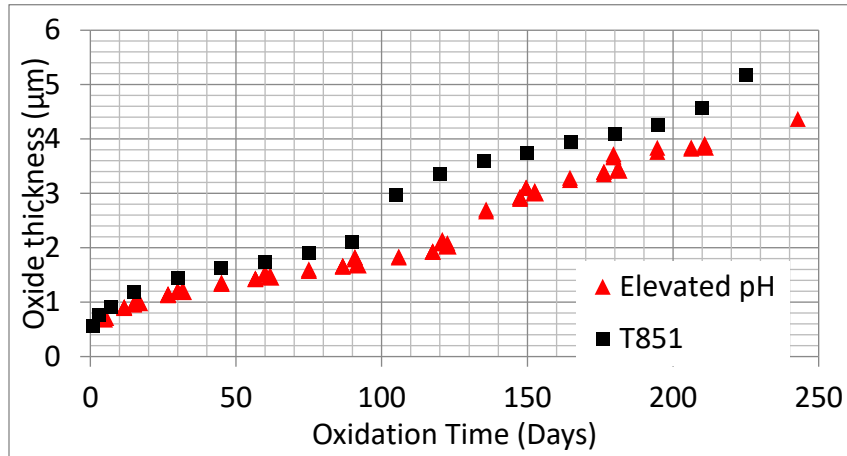
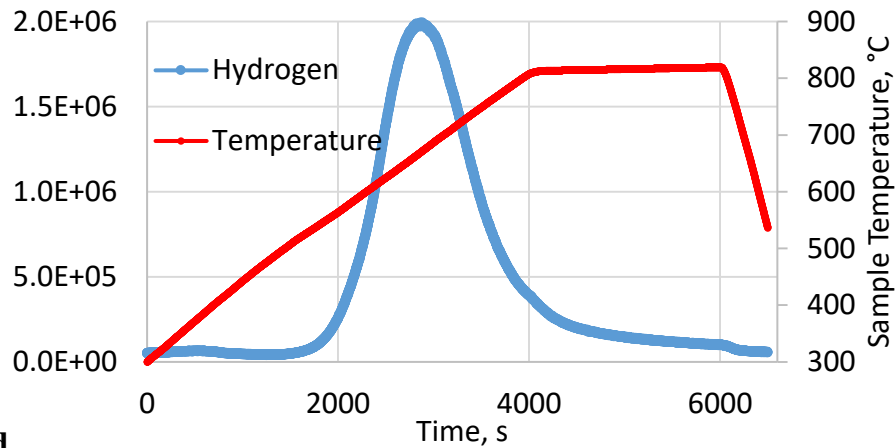


Figure 2 - Comparison of samples oxidized in pure water at 360°C vs samples oxidized in elevated pH at 350°C.

**Table 1** - Samples oxidized in elevated pH examined in this work (oxide thickness calculated from weight gain).

Oxidation Time (Days)	Oxide thickness (μm)
5	0.713
15	0.972
27	1.146
45	1.361
62	1.472
75	1.600
91	1.826
123	2.082
148	2.928
176	3.395
211	3.859
243	4.368

## RESULTS



### As-received

Figure 3 shows the hydrogen desorption spectrum from an as-received sample. The major peak is at 650°C, and a minor peak at 400°C. The 650°C peak has been characterised previously as the hydrogen released by the dissolution of hydrides in the metal<sup>1</sup>.

Samples of as-received material were run using different detector settings and different heating rates for calibration purposes. Figure 4 shows the effect of the emission current on the output spectra. The peak does not shift systematically with temperature, but the mass spectrometer response increases. Figure 5 plots the area of each spectrum from Figure 4 against the emission current, and clearly shows that the area of the spectra is proportional to the emission current. It also shows that the peak temperature is not affected by emission current.

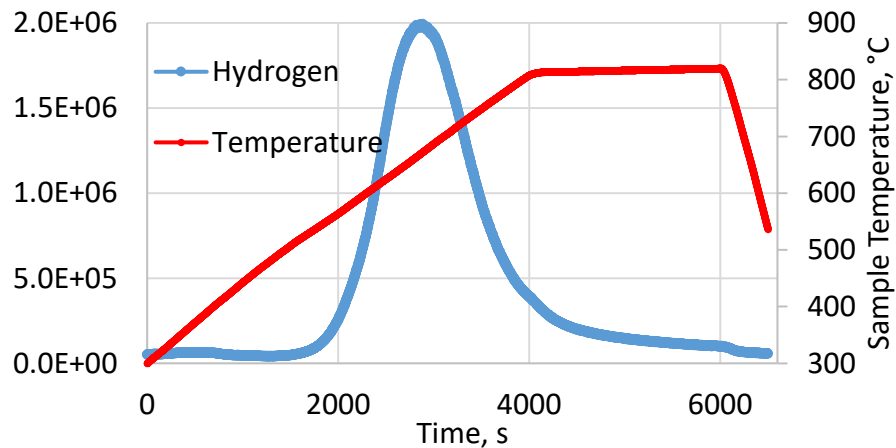


Figure 3 - Hydrogen desorption spectrum for an as-received sample heated at 10°C/min. The specimen surface temperature is measured from the right-hand axis. The left-hand y-axis is the response from the mass spectrometer, and is proportional to the amount of hydrogen evolved.

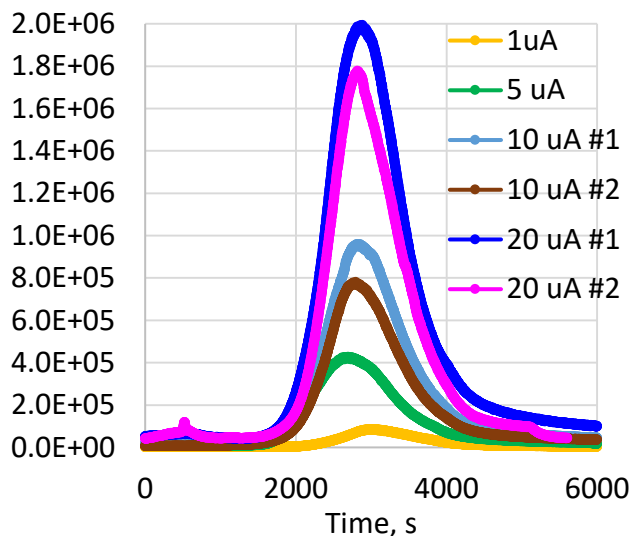


Figure 4 - Effect of emission current on desorption spectra. The heating rate was 10°C/min.

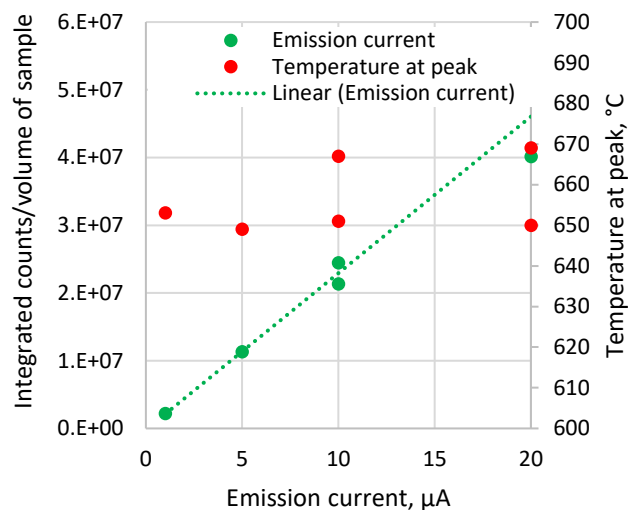


Figure 5 – Spectrum area per volume v emission current and temperature at peak

Figure 6 and Figure 7 show the effect of the heating rate on the desorption spectra. Decreasing the heating rate causes the peak to broaden, the peak value to decrease and the peak temperature to increase. The total amount desorbed did not vary significantly with heating rate.

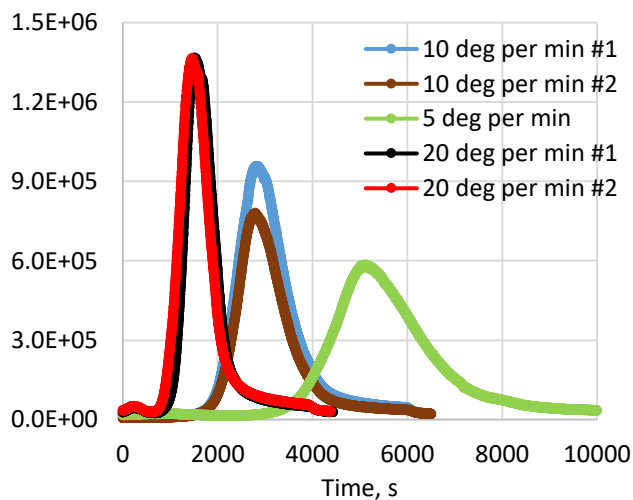


Figure 6 - Effect of heating rate on hydrogen desorption spectra. All were carried out with an emission current of 10  $\mu$ A.

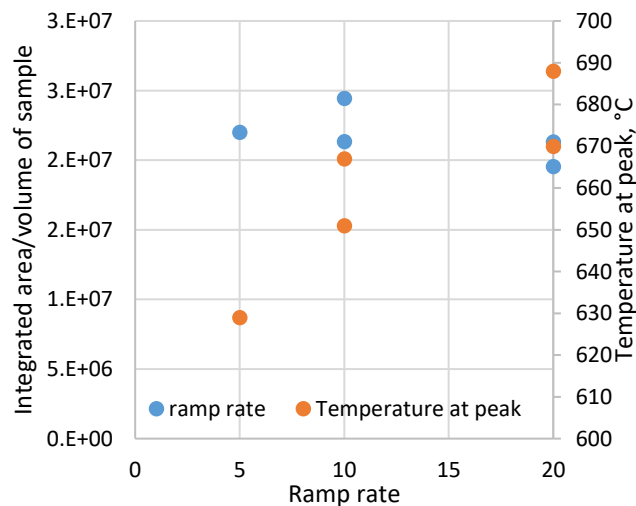


Figure 7 – Spectrum area per volume vs ramp rate, and temperature at peak.

### Cold rolled samples

Figure 8 and Figure 9 compare desorption spectra from the as-received sample shown in

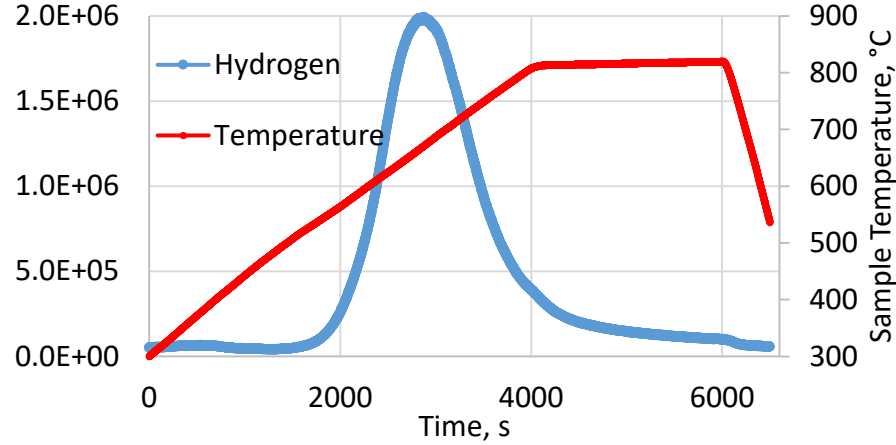


Figure 3 and two mechanically rolled samples. Cold rolling broadens the main peak and shifts it to lower temperatures (see Figure 9). It also increases the amount of hydrogen desorbed, although no deliberate H-charging was associated with the deformation. It is likely that the dislocations introduced by cold rolling provide a rapid diffusion path for the hydrogen, allowing it to reach the surface more rapidly, and from greater depths during the analysis.

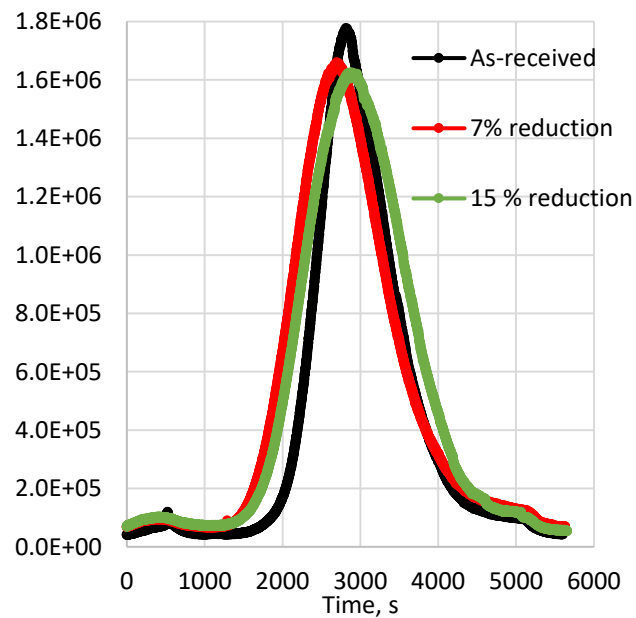


Figure 8 - Comparison of as-received sample to rolled samples. Notice the broadening of the peak in the rolled samples.

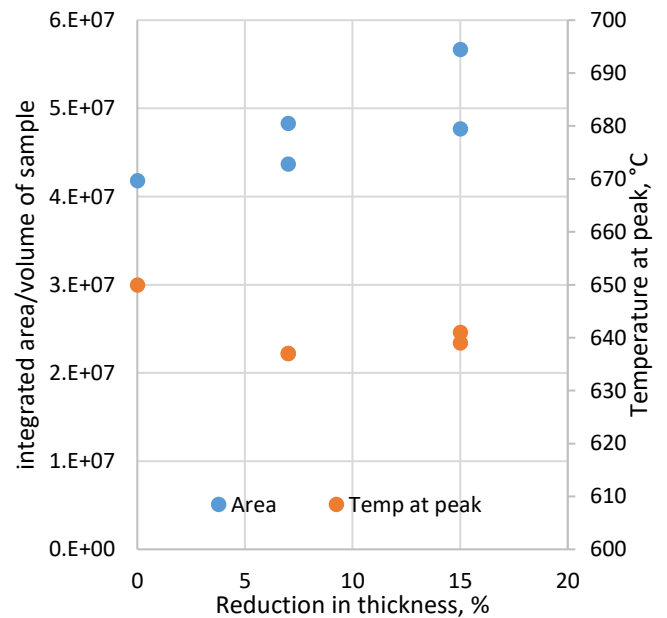


Figure 9 – Spectrum area per volume vs reduction in thickness, and temperature at peak.

### Hydrogen charged samples

Figure 10 shows the desorption spectra for samples electrolytically charged with hydrogen. The detector was set to the lowest sensitivity (1  $\mu$ A) as their high hydrogen content saturated the detector at any other setting. A spectrum from an as-received sample has been included, corrected for the emission current. No new peaks are produced, but the major peak increases in height and width, supporting the identification of this peak as relating to the hydrides. The peak also shifts to lower temperature with longer charging time, shown in Figure 11.

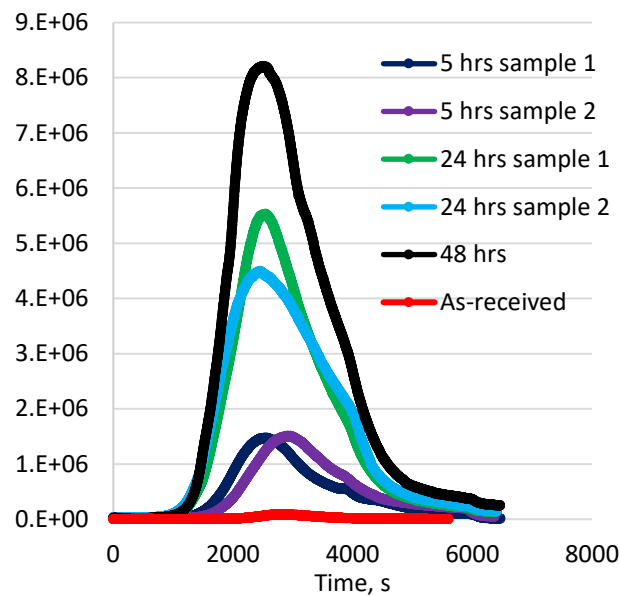


Figure 10 - Desorption Spectra for hydrogen charged samples. The as-received sample is the same as in Figure 3.

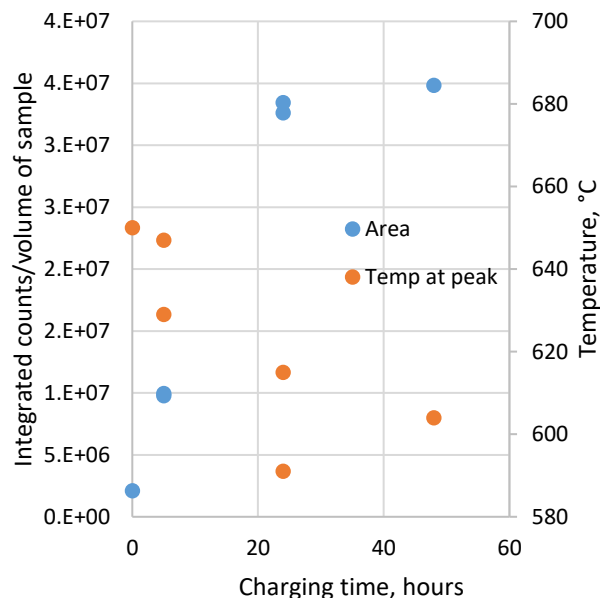


Figure 11 - Spectrum area vs charging time, and temperature at peak

### Impact of oxide on hydrogen desorption

Figure 12 shows the desorption graphs for samples oxidized for 45 days at elevated pH ( $1.36\mu\text{m}$ ), as removed from the autoclave, and with the oxide ground off prior to heating in the TDS. The heating curve of the sample with oxide (dark blue line) shows a slight overshoot before the surface settles to  $\sim 820^\circ\text{C}$ . The temperature is too low for the excess heat to be associated with the  $\alpha\beta$  phase transformation in the matrix. This overshoot is due to the exothermic dissolution of the oxide into the metal, as supported by the shiny metallic surfaces of the samples on removal from the TDS. Since few oxygen-containing species (i.e. no O, O<sub>2</sub>, NO, CO, CO<sub>2</sub>) are detected at this temperature, most of the oxygen appears to dissolve into the metal matrix.

In the absence of the surface oxide (red line), the hydrogen desorption peaks are at the temperatures seen in the previous plots ( $\sim 640^\circ\text{C}$  and  $330^\circ\text{C}$ ), indicating that no new trapping sites are produced in the metal by oxidation. In the presence of the oxide (light blue line), the peaks are shifted to higher temperatures. A burst of hydrogen is produced when the oxide dissolves. Calculating the area of these graphs shows that there is approximately the same amount of hydrogen in both samples ( $1.58 \times 10^7$  &  $1.74 \times 10^7$  for with and without oxide respectively), indicating that very little hydrogen is present in the oxide in comparison with the metal, in accordance with the lower solubility of H in the oxide<sup>13-15</sup>. The main effect of the oxide is to act as a diffusion barrier for the hydrogen desorbing from the metal.

The elevated pH environment contained 50% deuterated water, Figure 13 shows that D-H and D<sub>2</sub> desorption follows the same pattern as H<sub>2</sub> desorption, although the concentrations of these species are far lower than that of H<sub>2</sub>.

The desorption of oxygen-hydrogen species is shown in Figure 14. There are higher levels of the oxygen-hydrogen species in the sample from which the oxide was removed. The signals at low temperatures may relate to water adsorbed on the surface of the samples and the vacuum chamber as well as water deeper within the oxide. Hydrogen does, however, bond with oxygen in the oxide<sup>1,8,12</sup>. There is also a release around the same time that there is a burst of hydrogen from the sample, indicating that a small fraction of the oxygen in the oxide is desorbed with hydrogen rather than dissolved in the metal. It can also be seen that early on there is a release of HDO from the oxide, which is not present in the sample with the oxide removed. Comparison between the scales of Figure 12 and Figure 14 shows that the hydrogen desorbing in association with oxygen is more than an order of magnitude less than the hydrogen desorbing without oxygen.

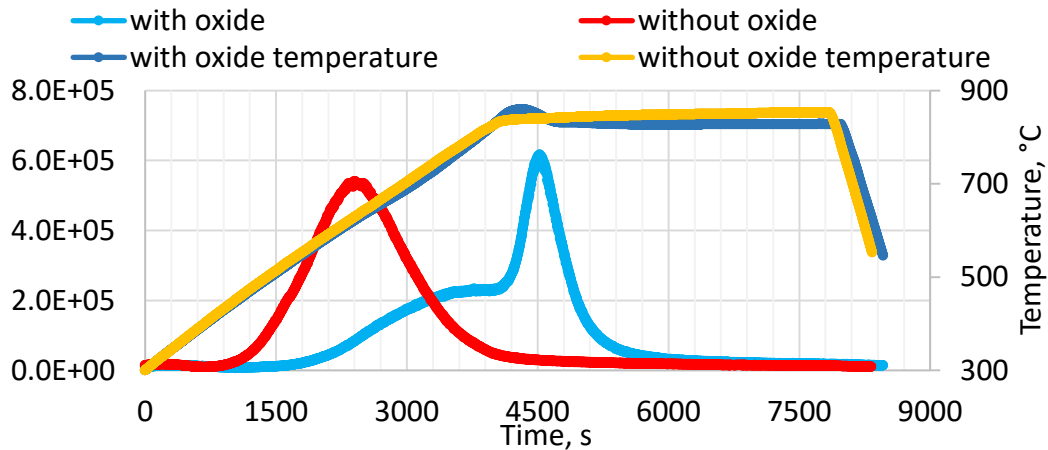


Figure 12 - Comparison of two samples oxidized for 45 days, with and without the oxide.

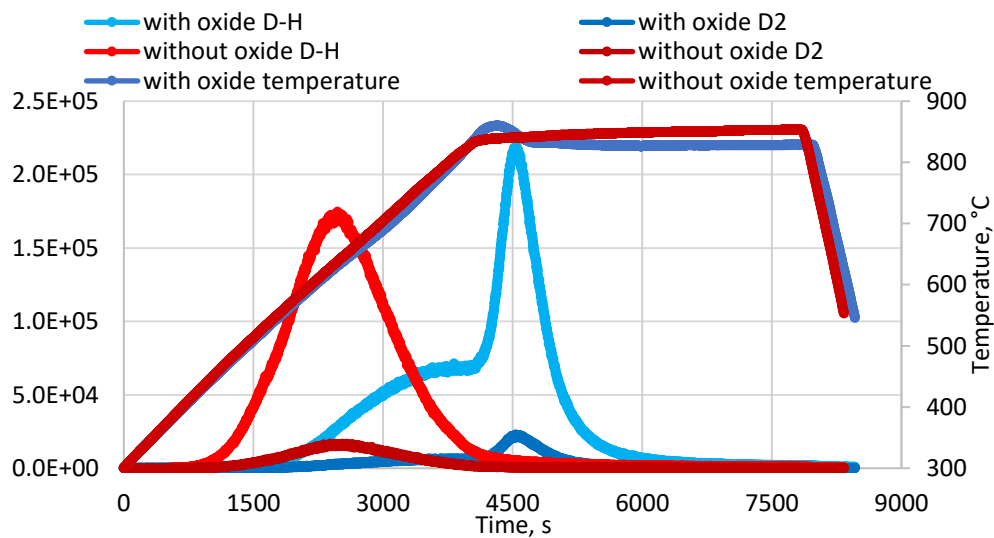


Figure 13 - D-H and D2 desorption from the same 45 day samples shown in Figure 12.

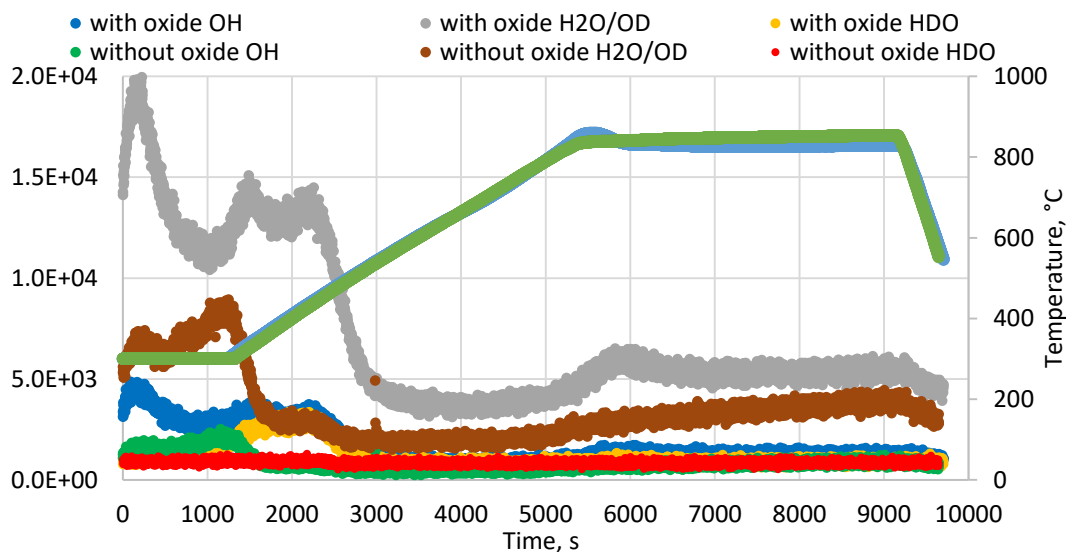


Figure 14 - Oxygen-hydrogen species desorbed by samples oxidised for 45 days.



### Effect of oxidation in water at different pH levels

Figure 15 compares the total hydrogen desorption from samples oxidized in pure water and at elevated pH. This shows that before transition the pH has little effect on the hydrogen pick-up. However after transition we see that while there is a slight increase (shown in more detail in Figure 16) for the high pH samples, there is a much larger increase for the pure water samples. It seems that a combination of the pH and the stage of oxidation are important in the hydrogen pick-up.

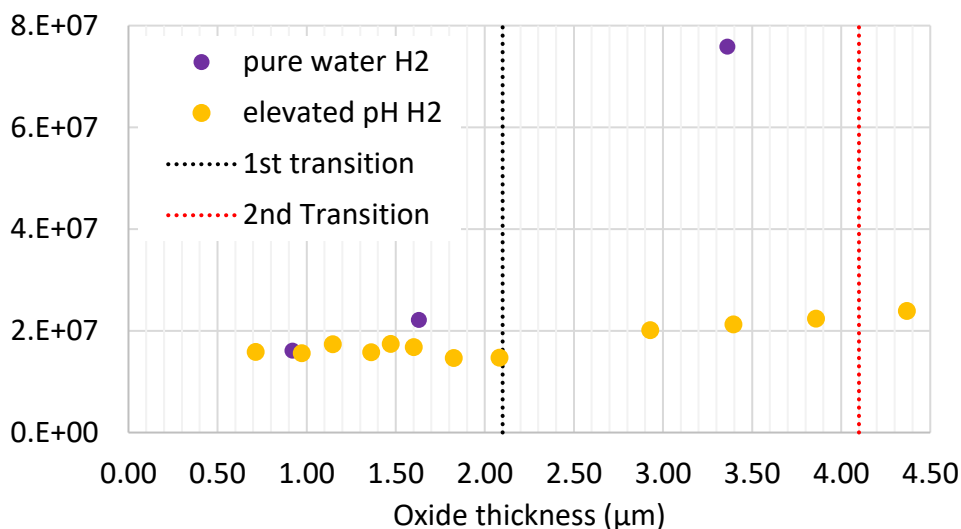


Figure 15 - Comparison of hydrogen desorption from samples exposed to different water chemistries.

### Hydrogen content of samples oxidized at high pH

Figure 16 shows the integrated areas for all the high pH samples, with and without the oxide present. Figure 17 shows a close up of the D<sub>2</sub> plots. The plots for all three species can be split into three regions:

1. Early pre-transition until 75 days.
2. Late pre-transition after 75 day up to transition ~120 days.
3. Post transition.

For region 1 it can be seen that, for all the species, the hydrogen/deuterium content either increases slightly (for D-H and D<sub>2</sub>) or stays roughly constant, regardless of the presence of the oxide layer. A reason that the H<sub>2</sub> count is consistently lower for the samples with the oxide present is that it loses more hydrogen as hydrogen-oxygen molecules (OH, H<sub>2</sub>O/OD, HDO).

For region 2 we see that the oxide layer has an influence. From all samples with the oxide still present, there is a significant reduction in the amount of all species detected. However, with the oxide removed we see that H<sub>2</sub> and D<sub>2</sub> increase although the D-H count decreases before increasing into transition.

For region 3 we see a large increase in all species from samples with the oxide present, and it can be seen that for H<sub>2</sub> the count becomes comparable (within error) to the H<sub>2</sub> count for samples with the oxide removed. For the oxide removed graph we see a plateau for H<sub>2</sub> and D<sub>2</sub> in region 3 before another sharp increase after 210 days (which could indicate that another transition has occurred).

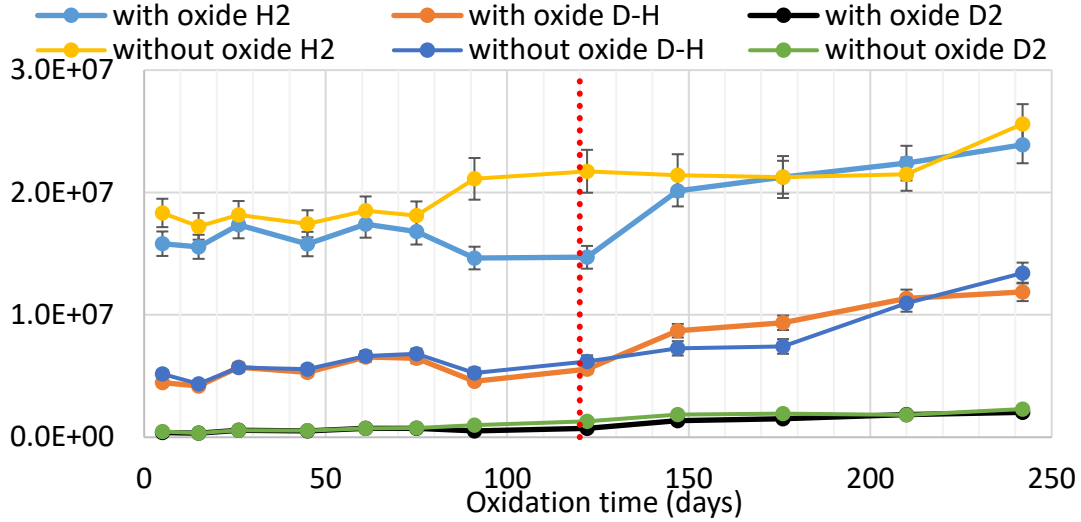


Figure 16 - Integrated counts for samples oxidised in an elevated pH, with and without the oxide present. The transition point is estimated to be 120 days and can be seen in Figure 2.

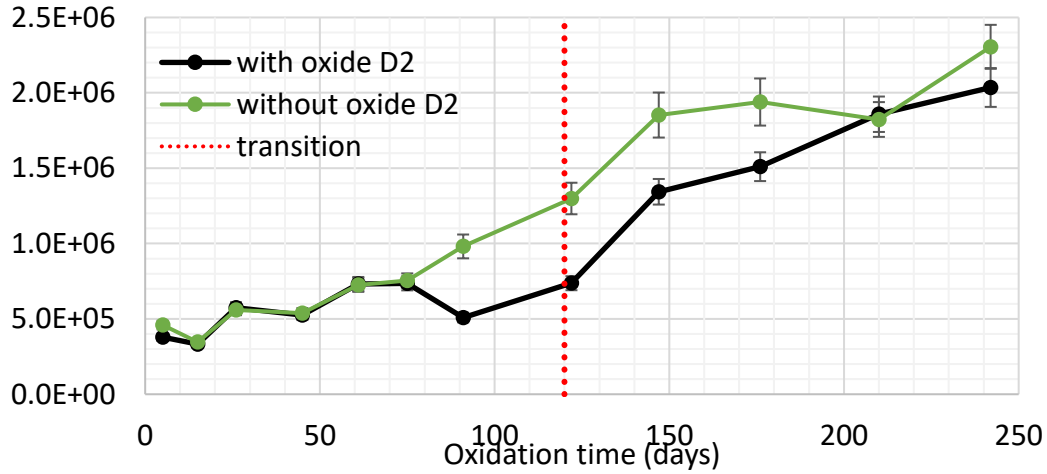


Figure 17 - D<sub>2</sub> plots from Figure 16.

To get a better understanding of how the hydrogen content varies across our samples we can look at the ratio of D<sub>2</sub> in the sample compared to H<sub>2</sub>. As there is D-H detected we need to take that into account. We used the following equation to compute the ratio:

$$\frac{D_2}{H_2} = \frac{([D_2]_d + \frac{[D-H]_d}{2})}{([H_2]_d + \frac{[D-H]_d}{2})} \quad (1)$$

Where  $[x]_d$  denotes the total counts for species  $x$  for oxidation time  $d$ . Figure 18 shows the plot of this ratio for all samples. Since the autoclave exposure was to 50% deuterated water while the natural abundance of D is around 0.01% this ratio shows us the hydrogen/deuterium pick-up during oxidation, as a function of the as-received hydrogen content. During the first five days of oxidation, the hydrogen pick-up rate is rapid, with the ratio showing (H<sub>2</sub>+D<sub>2</sub>) picked up exceeding a third of that originally present. From 5 days to transition, the amount picked up increases slowly, approaching two-thirds that originally present by transition. After transition the hydrogen pick-up increases steadily.

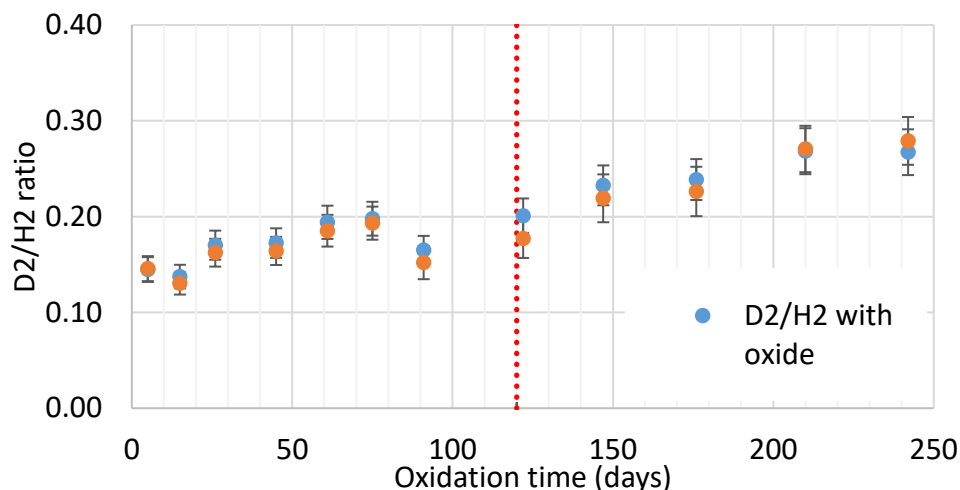


Figure 18 - D2 to H2 ratio.

### Conclusion

Thermal desorption of hydrogen from various Zircaloy-4 samples has been carried out, to determine trapping sites and how pH effects the hydrogen pick-up during oxidation. The main hydrogen desorption peak was around 650°C. This is fairly constant after cold rolling and hydrogen charging via electrolysis. Dislocations aid the diffusion of hydrogen from the metal while an oxide layer hinders it.

Increasing the pH of the oxidising water leads to a slightly lower oxidation rate and lower hydrogen pick-up after transition. It is possible that the change occurs shortly before or after transition. We will investigate this further to determine when the increase in the hydrogen pick-up occurs.

Although a small amount of hydrogen appears to be present in the oxide, the majority is found in the metal. It is not currently clear why such a drastic difference develops between the hydrogen desorbed from samples with/without oxide after 90 and 120 days.

The increase in hydrogen pick-up before transition might be related to the development of percolation paths through the oxide, which in turn could lead to the pH inside the cracks decreasing, so increasing the availability of  $H^+$  ions. This is still to be verified.

The data we have obtained so far only gives us a partial picture of what is happening. We intend to use rate theory modelling with the TMAP<sup>16</sup> code to compute the results to study the trapping energies and trapping sites in the metal and oxide.

### References

1. Chen, W., Wang, L. & Lu, S. Influence of oxide layer on hydrogen desorption from zirconium hydride. *J. Alloys Compd.* **469**, 142–145 (2009).
2. Berry, W. E., Vaughan, D. A. & White, E. L. Hydrogen Pickup during aqueous corrosion of zirconium alloys. *Corrosion* **17**, 109–117 (1961).
3. Yeniscavich, W., Wolfe, R. A. & Lieberman, R. M. Hydrogen absorption by nickel enriched zircaloy-2. *J. Nucl. Mater.* **3**, 271–280 (1959).
4. Motta, A. T. & Chen, L.-Q. Hydride Formation in Zirconium Alloys. *JOM* **64**, 1403–1408 (2012).
5. Couet, A., Motta, A. T. & Comstock, R. J. Hydrogen pickup measurements in zirconium alloys: Relation to oxidation kinetics. *J. Nucl. Mater.* **451**, 1–13 (2014).
6. Garzarolli, F., Cox, B. & Rudling, P. *ANT International Report: Corrosion and Hydriding*. (2012).
7. Harada, M., Wakamatsu, R., Limback, M., Kammenzind, B. & Dean, S. W. The Effect of Hydrogen on the Transition Behavior of the Corrosion Rate of Zirconium Alloys. *Zircon. Nucl. Ind. 15th Int. Symp. ASTM STP 1505* **5**, 101–117 (2008).

8. Peterson, W. J., Gilbert, R. E. & Hoflund, G. B. The interaction of Hydrogen with polycrystalline Zirconium Part II. The effect of preadsorbed oxygen. *Appl. Surf. Sci.* **24**, 121–124 (1985).
9. Eliaz, N., Eliezer, D., Abramov, E., Zander, D. & Koster, U. Hydrogen evolution from Zr-based amorphous and quasicrystalline alloys. *J. Alloys Compd.* **305**, 272–281 (2000).
10. Huang, J.-H. & Huang, S.-P. Hydriding of zirconium alloys in hydrogen gas. *Mater. Sci. Eng. A* **161**, 247–253 (1993).
11. Wongsawaeng, D. & Jaiyen, S. High-temperature absolute hydrogen desorption kinetics of zirconium hydride under clean and oxidized surface conditions. *J. Nucl. Mater.* **403**, 19–24 (2010).
12. Li, Y. S., Wong, P. C. & Mitchell, K. a. R. XPS investigations of the interactions of hydrogen with thin films of zirconium oxide II. Effects of heating a 26 Å thick film after treatment with a hydrogen plasma. *Appl. Surf. Sci.* **89**, 263–269 (1995).
13. Yamanaka, S., Fujita, Y., Uno, M. & Katsura, M. Influence of interstitial oxygen on hydrogen solubility in metals. *J. Alloys Compd.* **293 - 295**, 42–51 (1999).
14. Yamanaka, S., Nishizaki, T., Uno, M. & Katsura, M. Hydrogen dissolution into zirconium oxide. *J. Alloys Compd.* **293 - 295**, 38–41 (1999).
15. Miyake, M., Uno, M. & Yamanaka, S. On the zirconium–oxygen–hydrogen ternary system. *J. Nucl. Mater.* **270**, 233–241 (1999).
16. Longhurst, G. R. *TMAP7 User Manual*. (2004).